Volume 66, Issue 5, 2022
Journal of Scientific Research
of
The Banaras Hindu University

A Rician Noise Prediction and Removal Model for MRI Head Scans using wavelet based Non-Local Median Filter

T. Kalaiselvi[1], T. Anitha[1], Sriramakrishnan[2]
[1]Department of Computer Science and Applications, The Gandhigram Rural Institute (Deemed to be University), Gandhigram 624 302, Tamil Nadu, India. kalaiselvi.gri@gmail.com, anithat1892@gmail.com
[2]Department of Computer Applications, Kalasalingam Academy of Research and Education (Deemed to be University), Krishnankoil 626128, Tamil Nadu, India. sriram0210@gmail.com

Abstract: **In the medical imaging field, anatomical structure preservation is a difficult task during the denoising process. Magnetic resonance imaging (MRI) scanner corrupts the images by the Rician noise during the acquisition process. Rician noise affects the diagnosis and treatment planning for the subjects. Regenerating noise-free images is a time-consuming process with limited MR scanner resources available in developing countries. Therefore, the medical industry utilizes the advancement of computer-aided automatic denoising methods. This article presents a novel denoising method for Rician noise using a wavelet-based non-local median filtering (WNLMed) technique. The work contains three phases: noise estimation, wavelet thresholding using a lifting scheme, and non-local median filter (NLMed). Materials used for this experiment are collected from the Brainweb repositories and tested with validation metrics such as normalized absolute error (NAE), peak signal to noise ratio (PSNR), structure similarity index measure (SSIM), the figure of merit (FOM), and compared with the state-of-the-art methods. The method yields high PSNR value than other methods.**

Keywords

Denoising, Wavelet transformation, Lifting scheme, Soft thresholding, Rician noise, Non-local median.

I. INTRODUCTION

One of the most composite organs in our body is the brain. It consists of more than 10 billion neurons with 13 trillion connections with each other [1]. Due to its complex nature, the human brain's diagnosis is difficult in the medical field. There is different type of imaging techniques used in the medical field like computer tomography (CT), ultrasound, magnetic resonance imaging (MRI), x-ray, positron emission tomography (PET), and functional MRI (fMRI). MRI is a radiological technique that uses a magnet, radio frequency (RF) waves, and a computer to produce images. MRI is a more suggestible scanning procedure for the brain due to a non-invasive and non-ionizing ratio [2]. Also, MRI can detect brain conditions such as tumors, structural abnormalities, infections, inflammatory diseases, and blood vessel problems.

Noises lower the quality of medical images. Different types of noise appear in medical images, like substitutive noise, Rician noise, Poisson noise, and additive white Gaussian noise. Generally, denoising is essential before registration, restoration, enhancement, classification, segmentation, and volume construction. The filtering technique has two concepts, Linear and nonlinear (NL), which eliminate the noise from the homogeneous region.

Generally, MRI images are affected by Rician noise during the acquisition process [3]. Transverse magnetization produces these types of noise signals. Coupe et al. experimented using the standard volume coil to detect a noise model in MR images [4]. They observed that the noise in MR images is of Rician distribution. The magnitude value of an image's background regions is almost zero due to air particles known as Rayleigh noises. These noise artifacts reduce the visual image quality and make the diagnosis very difficult.

DIO: 10.37398/JSR.2022.660511

Fig.1. shows the MR Image and corrupted image by the Rician noise. The figure demonstrates that anatomical structure preservation is a difficult task during the denoising process.

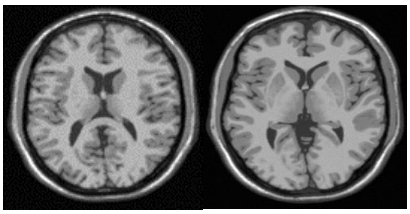

(a) (b)

Fig.1: MRI images a) clean MRI image b) Rician noise image

A wavelet is a small wave that represents both frequency and temporal information. Fourier transform uses smooth and infinite sine waves to break the signal. Unlike the Fourier transform, the wavelet splits the signal using an irregular wave function, making the wavelets an ideal tool for analyzing signals with discontinuity [5]. Wavelet transforms are performed by hard thresholding and soft thresholding based on their shrinkage rule. In hard thresholding, coefficients of noisy wavelets are set to zero. But the noisy wavelet coefficients are adjusted based on their subband coefficients in soft thresholding [6]. Compared to conventional Fourier transforms, wavelet transforms have certain advantages for expressing functions with sharp peaks, discontinuities, reconstructing and deconstructing signals. Fig. 2. Shows the types of wavelet transforms.

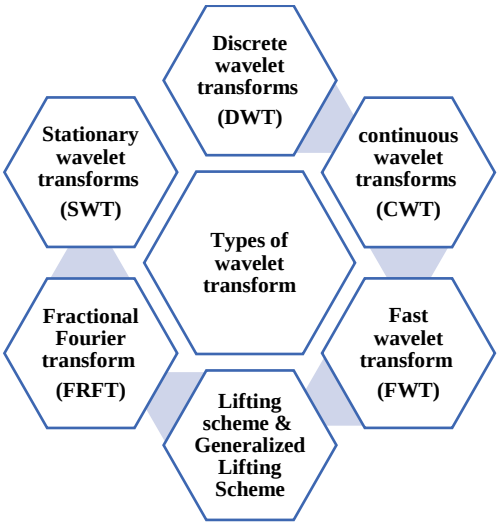

Fig. 2: Types of wavelet transform

The proposed WNLMed denoising method uses the lifting scheme wavelet transformation with a soft thresholding technique. Our method contains three phases: noise estimation, lifting wavelet scheme, and applying non-local median filter (NLMed). The first phase estimates the Rician noise level. The second phase produces the threshold image using multilevel wavelet thresholding with a lifting scheme. After the thresholding process, the inverse lifting wavelet transformation (IDWT) technique reconstructs the image. In the final phase, non-local median methods produce the denoised image from the reconstructed image. Materials used for this experiment are collected from the Brainweb repositories. The outcomes of our WNLMed approach are tested with validation metrics such as normalized cross-correlation (NCC), normalized absolute error (NAE), peak signal to noise ratio (PSNR), and compared with the existing denoising methods.

This paper is organized as follows. Section II presents the overview of existing approaches. Section III explains the theoretical background and properties of the lifting scheme wavelet transformation. Section IV introduces the methodology of the proposed work. Section V discusses materials and metrics used for the evaluation. Section VI discusses the outcomes of the proposed works. Section VII concludes the paper and discusses its potential scope.

II. COMPARATIVE METHODS

Bnou et al. have approached a denoising approach using wavelet techniques, an unsupervised learning model, and K-Singular Value Decomposition (K-SVD) algorithm [7]. Experiments are evaluated on standard images with performance metrics like SSIM and PSNR. Ferzo et al. have implemented a denoising technique to eliminate the noises that occur in the images. Here, wavelet domain, discrete wavelet transform technique(DWT), inverse DWT, and thresholding concepts are used with the Wiener filter to remove the Gaussian noise from the image [8]. Experiments are evaluated using a standard image with the performance metric PSNR. Chang et al. have developed a Bayeshrink technique with an optimal threshold using Baye's mathematical framework [9]. DWT is initially used to segregate the sub-bands and estimate the noise using a median absolute deviation (MAD) estimator. Here, the threshold value for each subband can reduce the noise with the threshold rule. This experiment has been carried out on standard images with Gaussian noise. Blu and Luisier had proposed a denoising method with stein unbiased risk estimation (SURE) and SURE linear expansion of thresholds (SURELET) [10]. They had applied a decimated wavelet transform to reduce the spatial information value. The pointwise thresholding function in a subband (HH) reconstructs the image by setting the subbands (HL & LH) as zero. Repeat the process for all levels, and then compute a matrix to find the optimal minimum SURE. Finally, noise-free images are generated by combining all reconstructed subbands with the weight.

Dengwen and Wengang have proposed an improved Neighshrink (INS) method with a fixed window size [11]. Initially, the image has transformed using a decimated wavelet

transform. The SURE procedure helps to set the window size and the local threshold value. At the end of this pipeline process, inverse decimated wavelet transforms (IDWT) support constructing noise-free images with superior denoising performance than SURELET. Budas et al. have extended a new neighborhood filter called non-local means (NLM) [12]. This filter worked with a window to analyze more similar pixels and periodic pixel patterns. The pixels lying in the window are scanned and searched for pixel patterns to be denoised. Finally, the noisy pixels are replaced with their original value. Shreyamsha has introduced an NLM filter and its noise thresholding (NLFMT) method [13]. NLM filter and wavelet thresholding can eliminate noisy components. Hence, DWT is applied to get more frequent subbands. Finally, they used Bayeshrink at low noise level subband and SURE thresholding in the subbands, which suffered from a high noise level. It gives less mean square error than existing methods and takes more computation time than others.

Kalaiselvi and karthigaiselvi have proposed an MRI denoising method based on the wavelet thresholding technique using a forward discrete Wavelet transform [14]**.** Using a noise estimator in each subband, the noisy wavelet coefficients are estimated from the original wavelet coefficients. For robustness, the K-means clustering technique is employed on the approximation section to get both background and foreground regions from the images. The noise level estimation in each subband helps to determine Baye's threshold value. In the thresholding, a new rule is regulated using the soft shrinkage rule. The rule considers that the wavelet coefficients, which have below the threshold value as noisy coefficients. In level two, the IDWT is performed after the shrinkage rule to get an image**.** They experimented with the IBSR website, and clinical data set and proved it better than the existing methods. The proposed WNLMed method outcomes are compared with the existing techniques discussed in this section.

III. BACKGROUND OF LIFTING SCHEME WAVELET TRANSFORMATION

Sweldens introduced a second-generation wavelet transform technique to perform the DWT) called a lifting scheme wavelet transformation. DWT utilizes several filters during the process. Constructing wavelet transformation involves the subsequent steps: in the primary step, data are divided into odd, and even sets; predicting phase predicts the odd set from even set and ensures that the polynomial cancellation in the high pass; update phase can update the even set using wavelet coefficient with scaling function and ensures the preservation of moments in low pass [15]. The basic form of a forward wavelet transforms, and inverse wavelet transform stated within the lifting scheme is shown in Fig. 3 and Fig.4 [16].

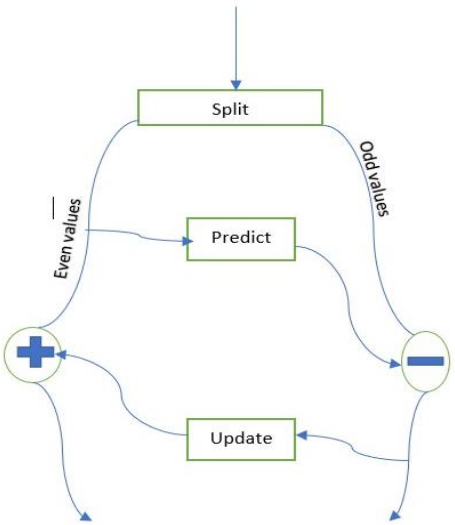

Fig.3: Forward lifting wavelet transforms

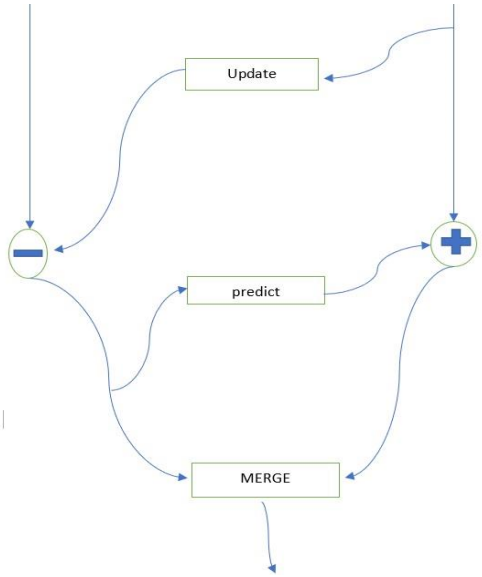

Fig.4: Inverse lifting wavelet transforms

Predict phase is denoted by *s,* and it is a high-pass filter. Wavelet functions and scaling functions are computed in the predict step and update step, respectively. Bi-orthogonal wavelets with the lifting scheme are used to improve the performance of DWT. The process of lifting and scaling is derived from bi-orthogonal wavelets, and the wavelet filters are written in the form of a polyphase matrix as given in Eqn. (1).

$$s(p) = \begin{bmatrix} m_{even}(p) & l_{even}(p) \\ m_{odd}(p) & l_{odd}(p) \end{bmatrix} \qquad (1)$$

where, dets(p) $= p^{-k}$ and the 2 × 2 polyphase matrix contains

the low-pass filter and high-pass filters. Each filter is normalized and divided into its even and odd polynomial coefficients. The matrix factor is produced as 2 × 2 upper and lower triangular matrices when diagonal entries are equal to 1. The factorization of the polyphase matrix is given below in Eqn. (2).

$$s(p) = \begin{bmatrix} 1 & q(1+p^{-1}) \\ 0 & 1 \end{bmatrix} \begin{bmatrix} 1 & 0 \\ t(1+p) & 1 \end{bmatrix} \quad (2)$$

the coefficients in the predict and update steps are d and e, respectively.

Based on the matrix theory, a matrix with determinant and polynomial entries can be factored in the form of multistep given in Eqn. (3) with predicts, update, and scaling steps.

$$s(p) = \begin{bmatrix} 1 & q(1+p^{-1}) \\ 0 & 1 \end{bmatrix} \begin{bmatrix} 1 & 0 \\ t(1+p) & 1 \end{bmatrix}$$

$$\begin{bmatrix} 1 & f(1+p^{-1}) \\ 0 & 1 \end{bmatrix} \begin{bmatrix} 1 & 0 \\ t(1+p) & 1 \end{bmatrix} \begin{bmatrix} r_1 & 0 \\ 0 & r_2 \end{bmatrix} \quad (3)$$

The second prediction step coefficient is f, and t is assigned as a coefficient for the second update step. The coefficient of odd-sample scaling is r_1 and r_2.

For the denoising process, we used the wavelet transformation based on the lifting scheme (LS). Because of the following advantages of the wavelet transform [17]:

(i) The computation time of LS is faster than convolution-based DWT, and no auxiliary memory is required.
(ii) In-place calculation of the wavelet transform is allowed in LS.
(iii) Compared to floating-point numbers, LS is more comfortable storing and process integer numbers.

IV. PROPOSED METHODOLOGY

The proposed work contains eight steps to obtain a denoise image using Brainweb dataset images. The procedure of the proposed work is short out based on given Algorithm 1.Figure 5 shows the block diagram of our WNLMed method.

Algorithm 1: Step by step process of the proposed method

Phase 1: Noise estimation

Step 1: Input: Brainweb MRI images.

Step 2: Apply the Rician noise and Estimate the noise

Phase 2: Wavelet thresholding using a lifting scheme

Step 3: Apply Lifting Forward wavelet transform

Step4: Threshold detection

Step 5: Apply shrinkage rule (Soft thresholding)

Step 6: Apply to lift Inverse wavelet transform

Phase 3: Non-local median filter (NLMed)

Step 7: Apply the Non-local median filter to the wavelet image.

Step 8: Output: denoised image.

A. Phase 1: Noise estimation

We have taken the clear MRI images from the Brainweb dataset and added Rician noise to the original MRI images based on the Coupe et al.[4] algorithm as well as estimates the noise level. The consequence of noise estimation (sigma) is one of the parameters for the phase three process.

B. Phase 2: Wavelet thresholding using a lifting scheme

Apply the Lifting forward wavelet transform to the noisy image by using lwt2 in db8. Daubechies (db8) is one of the wavelet families. Before denoising, thresholding plays a significant role, and hard thresholding (Thr_H) can be defined as:

$$\boldsymbol{Thr_H} = \begin{cases} \boldsymbol{x}; & \boldsymbol{for\ |a| \geq tv} \\ \boldsymbol{0}; & \boldsymbol{in\ all\ other\ regions} \end{cases} \quad (4)$$

Where $\boldsymbol{tv}$ is the value of the threshold, and $\boldsymbol{a}$ is the coefficients of magnitude. When coefficients of magnitude are more significant than $\boldsymbol{tv}$ then remaining are set to zero.

Assume that the coefficients are **more significant** than the threshold then shrink towards zero [19]as defined as follows:

$$\boldsymbol{Thr_S} = \begin{cases} \boldsymbol{sign(a)(|a| - tv),} & \boldsymbol{for |a| > tv} \\ \boldsymbol{0,} & \boldsymbol{in\ all\ other\ regions} \end{cases} \quad (\mathbf{5})$$

From the observation, soft thresholding produces a more visually pleasant image, whereas hard thresholding yields abrupt artifacts in the image. Soft thresholding produces less mean square error (MSE). Therefore, our WNLMed method utilizes soft thresholding. After thresholding, ILWT is placed to get the level 1 lifting wavelet threshold image by using ilwt2 in db8.

Phase 3: Non-local median filter (NLMed)

After ILWT, NLMed is applied for the denoising phase. The ILWT image's output will be the input of the NLMed process, and the noise estimation value (sigma) is used as one of the parameters. NLM is a neighborhood processing, and it computes weighted means between-patch dissimilarity measure proposed by Buades et al. [12]. The proposed modified NLMed utilizes the NLM and Chaudhury algorithm

[12, 20]. The procedure of this NLMed algorithm is discussed below.

The non-local median filter's basic principle is to replace each pixel's gray level with the median of the grayscale level in neighbor pixels, using the median operation based on the defined window size (patch size) [21]. Before starting the NLMed filtering, zeros must be padded around the row edge and the column edge.

The traditional median filter removes low-level noise from the image, but it is not good at high-level noise. Here, sizes of windows are 3×3, 5×5, 7×7, and 9×9 to remove a high-level noise from the medical images [22].

Algorithm 3: Algorithm of NLMed

Step1: Input: ILWT image $x = x_l$ and parameters p, sw, w
Step2: Output: Denoised image $\hat{x} = (\widehat{x_l})$.
1. Extract patch p_l of size w × w at each pixel l.
2. For each pixel l do
a. define $w_{lm} = \exp\left(-\frac{\|p_l - p_m\|2}{h^2}\right)$ for each m € sw(l).
b.Find patch p that minimizes $\sum_{m \in sw(l)} w_{lm} ||p - p_m||$
c.Assign $\hat{x} = (\widehat{x_l})$ the value of the center pixel in p.
3. Output Image : denoised image as $\hat{x} = (\widehat{x_l})$.

V. MATERIALS AND METRICS

The tests are performed in the MRI volumes from the Brainweb dataset [23]. The dataset contains a group of real brain volumes formed by an MRI simulator. This dataset includes T1, T2, and proton-density (PD) weighted 3-D data volumes and a level of intensity non-uniformity, the slice thicknesses, noise levels. We can view the dataset in three orthogonal views such as transversal, sagittal, and coronal. It has T1 Modality, ICBM Protocol, normal phantom, Slice thickness as1mm, 0% noise, with 181 slices. Each slice has 181 pixels' width and 217 heights. Each pixel has 88 dpi horizontal and vertical resolution.

The metrics are used for quantitative validations for comparing the performance. The following metrics are used to evaluate our WNLMed method performance: PSNR, NAE, SSIM, and FOM.

PSNR (Peak-Signal-to-Noise-Ratio) estimates the ratio between original and noisy signals. It is computed by the mean squared error (MSE) and measured in the logarithmic decibel scale. The quality of the image improves when the MSE value is decreased [24].

$$PSNR = 10log_{10}\left(\frac{MAX^2}{MSE}\right) \quad (6)$$

$$MSE = \frac{1}{mn}\sum_{i=0}^{m-1}\sum_{j=0}^{n-1}[I(i,j) - K(i,j)]^2 \quad (7)$$

Let MAX denotes the value of maximum intensity in the image.

NAE (Normalized Absolute Error) is the entire absolute error normalized by the error simply predicting the standard of the actual values. Minimized value of NAE shows the quality image. This quality measure can be expressed as follows.

$$NAE = \frac{\sum_{i=1}^{m}\sum_{j=1}^{n}(|A_{ij} - B_{ij}|)}{\sum_{i=1}^{m}\sum_{j=1}^{n}(A_{ij})} \quad (8)$$

SSIM(Structure Similarity Index Measure) measures the similarity between two images [25]. The perceptual quality of the images is characterized by the SSIM based on the available structural information by the following equation 9.

$$SSIM = \frac{(2\mu_x\mu_y + c_1)(2\sigma_{xy} + c_2)}{(\mu_x{}^2 + \mu_y{}^2 + c_1)((\sigma_x{}^2 + \sigma_y{}^2 + c_2)} \quad (9)$$

Where,μ_x-the average of x, μ_y - the average of y, $\sigma_x{}^2$- the variance of x, $\sigma_y{}^2$-the variance of y, σ_{xy} - the covariance of x and y.

FOM(Figure of Merit) is used for quantitative comparison edge preservation algorithms in image processing. We use Pratt FOM (PFOM) method to validate the edge preservation outcomes of our proposed method. PFOM is determined by the mathematical expression given in equation 10. The PFOM measures the outcome value of detected edges between 0 and 1. when the outcome value gets near to 1; it shows that detected edge outcomes are better [26].

$$FOM = \frac{1}{\max(N_{ED}, N_{OI})}\sum_{1}^{N_{OI}}\frac{1}{1 \times \alpha \times d_i^2} \quad (10)$$

Where,N_{ED}, $number\ of\ actual\ Edges$, N_{OI} – $number\ of\ detected\ edges$, d_i^2 denotes the distance between the actual edge and the detected edge. α is scaling constants set to 1/9.

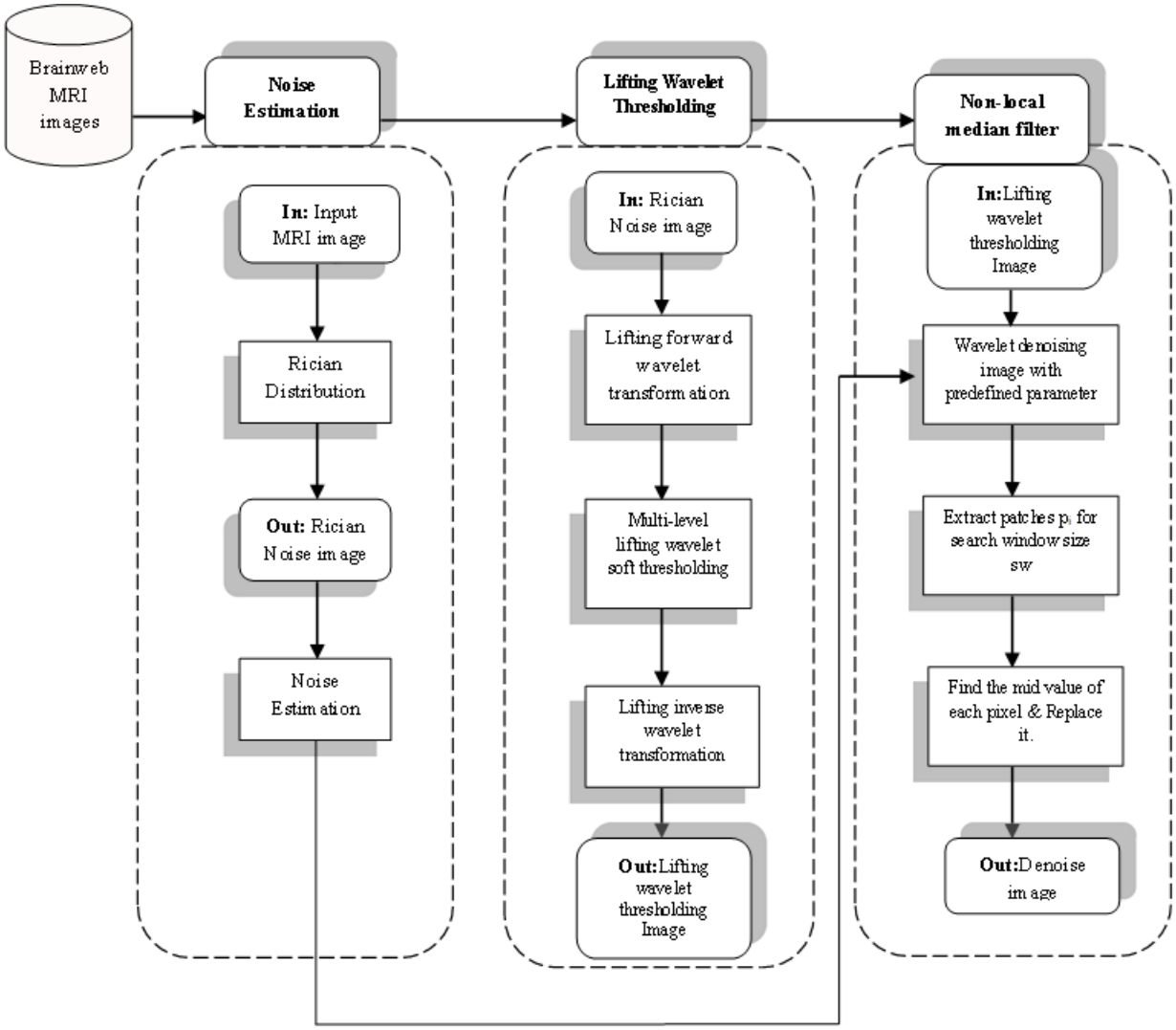

Fig. 5: Block diagram of the proposed method

VI. RESULTS AND DISCUSSION

Our WNLMed work is implemented in Matlab R2018a using Brainweb dataset images. The experiments were performed in the Intel CORE i3 processor with 8GB RAM and Windows 10 operating system platform. This work generates denoised images using the lifting scheme with soft thresholding and a non-local median filter. The outcomes are compared with some of the existing methods such as novel wavelet thresholding (NWT),non-local filter using Wavelet (NLFMT), Bayeshrink, and Improved Neigh Shrink with SURE (INS) unbiased estimation[14]. Performances of the proposed and existing works are compared with PSNR, NAE, SSIM, and FOM.

Table 1 - Table 4 gives quantitative results derived from the qualitative analysis depicted in Figure 6 - Figure 16. The evaluation starts with a lower level of Rician noise level. At first, 2 % Rician noise has been applied to the MRI brain image and denoised by the proposed WNLMED technique and shown in Figure 6. In this figure, 6(a) is the original image, 6(b) is the noisy image, 6(c) is a denoised image by lifting wavelet scheme, and 6(d) shows the denoised image by WNLMED technique. Likewise, the proposed work has been evaluated for the 6 % and 15 % of the Rician noise and shown in Figure 7 and Figure 8. From this, our proposed work gives a better result than lifting wavelet images.

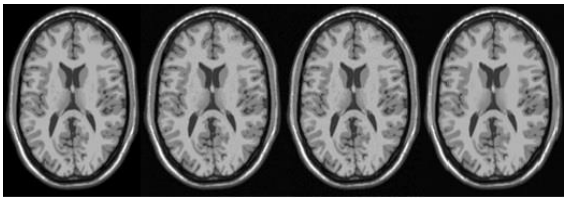

(a) (b) (c) (d)

Fig. 6: Qualitative outcomes of our WNLMed method for 2% of noise level (a) clean image (b) Noisy image (c) Lifting wavelet Image (d) WNLMed denoised image.

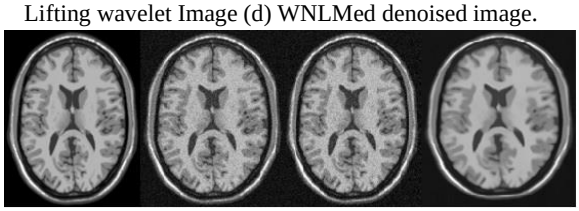

(a) (b) (c) (d)

Fig. 7: Qualitative outcomes of our WNLMed method for 6% of noise level (a)clean image (b) Noisy image (c) Lifting wavelet Image (d) WNLMed denoised image.

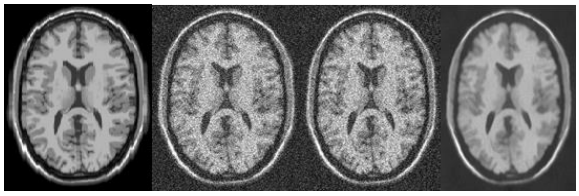

(a) (b) (c) (d)

Fig. 8: Qualitative outcomes of our WNLMed method for 15 % of noise level (a)clean image (b) Noisy image (c) Lifting wavelet Image (d) WNLMed denoised image.

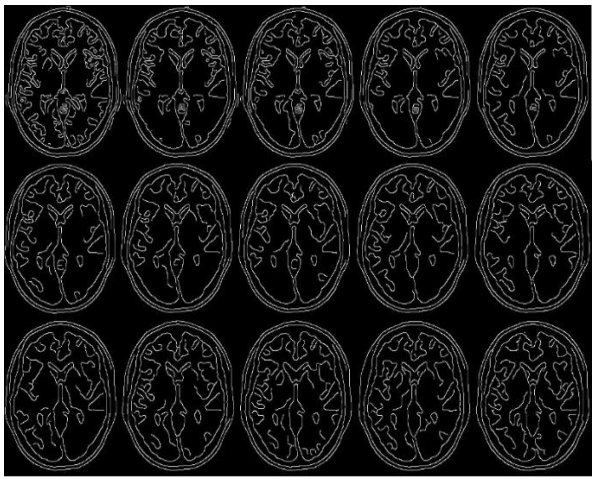

Fig. 9: Qualitative outcomes of our WNLMed method edge image for 2 to 15 % of noise level (a)clean Edge image (b) WNLMed denoised edge image for 2 to 15% noise level.

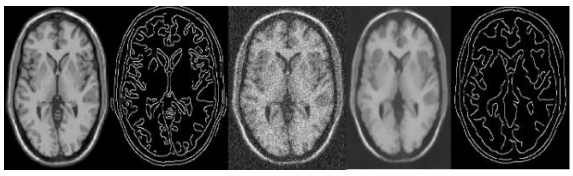

(a) (b) (c) (d) (e)

Fig. 10: Qualitative outcomes of our WNLMed method image for 15 % of noise level (a) Clean image (b)clean Edge image (c) 15 % noisy image (d) WNLMed denoised image (e) WNLMed denoised edge image.

The test has been done by applying various levels of Rician noises (2% to 15%) shown in Table 1 and examining existing works with our WNLMed methods. Table 1 illustrates that our WNLMed work produces better outcomes in 15% of the noise level. The performance of our WNLMed method is improved when the presence of noise is increased. Our WNLmed method works well for higher noise ratios.

We use the soft thresholding technique for our proposed work because soft thresholding gives a better result than a hard thresholding technique. Table 2 and Table 3 compare the lifting wavelet denoising image with our proposed work using the soft thresholding technique and hard thresholding technique. From the tables, we analyze that our proposed work yields better results. In our method, first, we use the lifting wavelet technique for denoising the MRI images. It does not remove the noise from the MRI images. So we move to a non-local median filter concept to eliminate the Rician noise from the images. We know that the median filter is one of the edge-preserving techniques. The preprocessing image of lifting wavelet denoising is passed to stage 2 processes as an input with some predefined parameters to produce better results. From table 2, we see that the PSNR value of the wavelet image will be lower than the lifting wave NLM value.

In our proposed work, we use the sigma as one of the parameters in the stage 2 process; here, sigma is the estimation of noise applied in the MRI image. Table 4 consists of the Rician noise level and their noise estimation applied in the Brainweb images. Fig.9 and Fig.10 show the qualitative results of our proposed work using the soft and hard thresholding technique to prove that the soft thresholding method produces better outcomes than the hard thresholding method. Fig.11 and Fig.12 provide a clear difference between both methods.

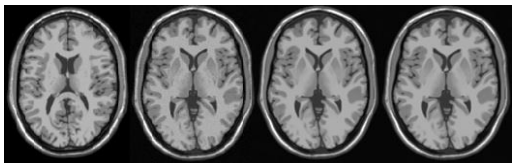

(a) (b) (c) (d)

Fig.11: shows the difference between the soft thresholding and hard thresholding for noise level 2 % a) Clean image b) noisy image c) soft thresholding image d)hard threshold image.

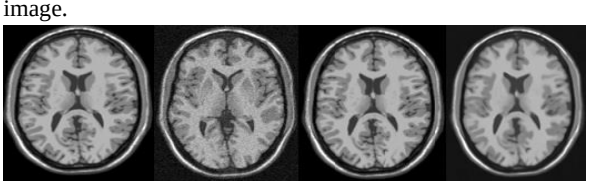

(a) (b) (c) (d)

Fig.12: shows the difference between the soft thresholding and hard thresholding for noise level 6 % a) Clean image b) noisy image c) soft thresholding image d) hard threshold image.

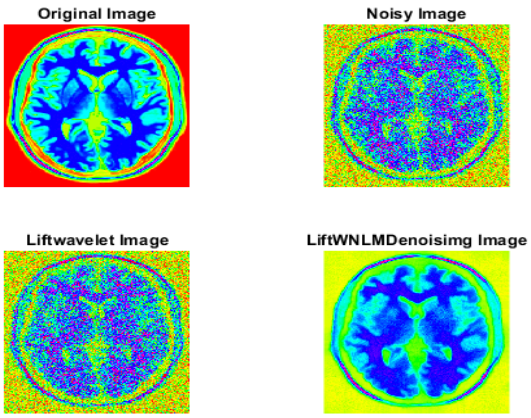

Fig.13: Denoised image using lifting WNLMEd filter with soft thresholding technique

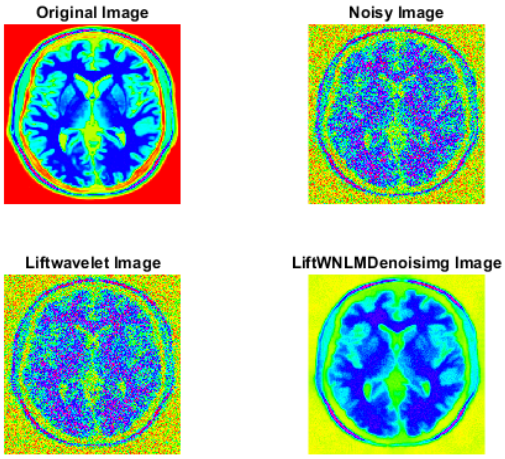

Fig.14: Denoised image using lifting WNLMEd filter with hard thresholding technique.

Table 1: PSNR value of our WNLMed method with the existing method with noise level 2% to 15%

Noise Level (%)		**2**	**3**	**4**	**5**	**6**	**7**	**8**	**9**	**10**	**11**	**12**	**13**	**14**	**15**
PSNR (dB)	**Bayes[14]**	40.41	33.98	30.22	25.55	23.9	22.52	21.53	20.28	19.34	19.29	18.51	17.8	17.14	16.53
	INS[14]	41.45	35.71	32.27	27.88	26.3	24.95	23.78	22.74	21.8	19.65	18.88	18.16	17.5	16.89
	NLFMT[14]	41.52	31.71	29.53	27.06	25.59	24.44	23.38	22.45	21.54	19.56	18.77	18.05	17.41	16.8
	NWT	39.9	35.36	32.14	27.91	26.37	25.01	23.97	22.79	21.86	20.02	19.25	18.52	17.86	17.24
	Proposed	40.07	35.22	32.36	30.08	28.19	26.58	25.31	24.21	23.22	22.3	21.5	20.04	19.44	18.89

Table 2: PSNR and NAE values of Lifting Wavelet image and lifting wavelet NLM image using soft thresholding

Noise Level (%)		**2**	**3**	**4**	**5**	**6**	**7**	**8**	**9**	**10**	**11**	**12**	**13**	**14**	**15**
Lift-Wave(S)	**PSNR**	32.80	29.27	26.87	24.89	23.334	22.035	20.89	19.82	18.88	18.08	17.38	16.67	16.05	15.44
	NAE	0.051	0.078	0.103	0.129	0.155	0.180	0.205	0.233	0.259	0.284	0.308	0.334	0.359	0.386
Proposed(S)	**PSNR**	40.07	35.22	32.36	30.08	28.19	26.58	25.31	24.21	23.22	22.30	21.50	20.73	19.44	18.89
	NAE	0.023	0.039	0.053	0.068	0.0845	0.101	0.117	0.133	0.148	0.166	0.182	0.198	0.23	0.245

Table 3: PSNR and NAE values of Lifting Wavelet image and lifting wavelet NLM image using hard thresholding

Noise Level (%)		**2**	**3**	**4**	**5**	**6**	**7**	**8**	**9**	**10**	**11**	**12**	**13**	**14**	**15**
Lift-Wave(H)	**PSNR**	33.09	29.54	27.05	25.13	23.53	22.18	21.06	20.07	19.12	18.33	17.55	16.90	16.23	15.65
	NAE	0.0503	0.075	0.101	0.126	0.151	0.177	0.200	0.225	0.251	0.275	0.301	0.324	0.351	0.374
	PSNR	**35.64**	32.67	30.31	28.38	26.83	25.47	24.47	23.49	22.60	21.78	20.99	20.43	19.69	19.16
	NAE	**0.036**	0.050	0.065	0.082	0.097	0.113	0.128	0.143	0.159	0.173	0.191	0.203	0.222	0.236

Table 4: Rician Noise Estimation of desired noise level applied for Brainweb images

Noise Level(%)	Noise Estimation (Sigma)
2	4.84
3	7.14
4	9.51
5	11.71
6	14.09
7	16.36
8	18.59
9	20.79
10	23.17
11	25.14
12	27.33
13	29.34
14	31.59
15	33.79

.

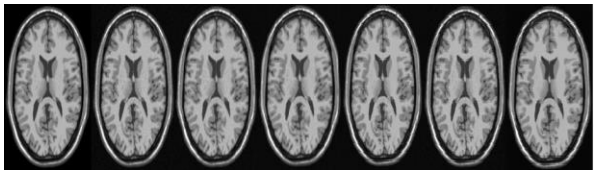

(a) (b) (c) (d) (e) (f) (g)

Fig. 15: Qualitative outcomes of our WNLMed method with existing methods for 2 % of noise level (a)clean image (b) Noisy image (c)Bayes (d)INS (e)NLFMT (f) NWT (g) WNLMed denoised image.

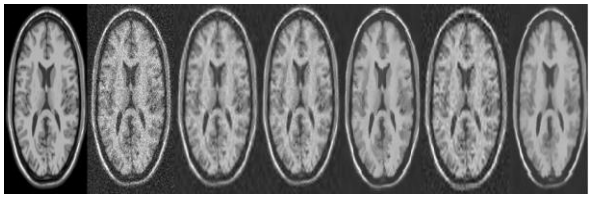

(a) (b) (c) (d) (e) (f) (g)

Fig. 16: Qualitative outcomes of our WNLMed method with the existing methods for 15 % of noise level (a) clean image(b) Noisy image (c)Bayes (d)INS (e) NLFMT (f) NWT (g) WNLMed denoised image.

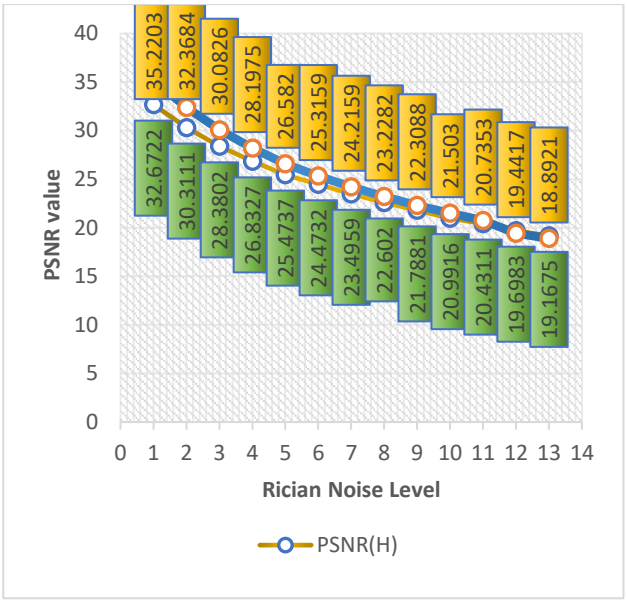

Fig.17: Comparison between soft Thresholding and Hard Thresholding techniques.

The proposed method's qualitative results are shown in Fig. 6,7, and 8 for the noise levels 2%, 6%, and 15 %. Figures show the comparative results of clean image and noisy image with lifting wavelet transformation image and lifting wavelet non-local median filter images.

Figure 13 and 14 shows the comparative results of our WNLMed method with some of the existing methods like Bayes, INS, NLFMT, NWT for the noise level 2% and 15 %[12]. Both figures 13 and 14 show that our WNLMed work yields better results and preserves the existing methods table 5 shows the SSIM and FOM values of the proposed method.

Fig.15 shows the diagrammatic difference between soft and hard thresholding techniques. Time consumption is the most important requirement in the medical imaging field. So that we compared the time complexity of our proposed work with existing methods like Bayes, INS, NLFMT[14]. Table 6 clearly shows the time complexity difference of our proposed method with existing methods. In table 6 Bayes method has less computational time than our proposed work but their qualitative outcome is not better than our qualitative outcomes.it is shown in Figures 13 and 14. From the above qualitative and quantitative outcomes we state that our proposed work yields better results than comparative methods.

Table 5: SSIM and FOM values of a Proposed method for Rician noise level 2% to 15%.

Noise Level (%)	**2**	**3**	**4**	**5**	**6**	**7**	**8**	**9**	**10**	**11**	**12**	**13**	**14**	**15**
SSIM	0.9987	0.9984	0.9981	0.9979	0.9978	0.9975	0.9973	0.9973	0.9971	0.9969	0.9969	0.9969	0.9967	0.9967
FOM	0.9072	0.8559	0.8329	0.8303	0.8226	0.7854	0.7561	0.7592	0.7616	0.7553	0.7822	0.7968	0.7632	0.7846

Table 6: Computational Time of a proposed method and existing method for Rician noise level 2% to 15%.

Noise Level(%)		**2**	**3**	**4**	**5**	**6**	**7**	**8**	**9**	**10**	**11**	**12**	**13**	**14**	**15**
Time (sec.)	**Proposed**	140.9	137	137	134.9	136.4	143.5	150	142.3	141	139	137.6	142	144.8	138.1
	Bayes	20.16	20.34	19.22	19.19	19.71	19.58	20.12	19.64	19.62	19.80	19.79	19.61	19.74	19.90
	INS	389.85	408.78	401.72	401.66	392.65	403.25	394.83	397.05	395.25	412.53	420.02	420.74	414.21	411.99
	NLFMT (mins)	235	232	222	224	221	234	255	240	244	260	235	232	224	231

VII. CONCLUSION

In this paper, we have developed a wavelet-based denoising technique using the NLMed (WNLMed) approach. The experiments were done with Brain web data, and the results were compared with existing systems using the metrics. The results show that our approach yields better consequences than several existing techniques with a high noise ratio. In the future, we will improve the implementation of our work to achieve better qualitative and quantitative outcomes than now with minimum computational time.

REFERENCE

[1] Kalaiselvi, T. "*Brain portion extraction and brain abnormality detection from magnetic resonance imaging of human head scans*." Pallavi Publication (2011).

[2] Kalaiselvi, T., P. Kumarashankar, and P. Sriramakrishnan. "*Three-Phase Automatic Brain Tumor Diagnosis System Using Patches Based Updated Run Length Region Growing Technique*." Journal of digital imaging (2019): 1-15.

[3] Kalaiselvi, T., and S. KarthigaiSelvi. "*Investigation of Image Processing Techniques in MRI Based Medical Image Analysis Methods and Validation Metrics for Brain Tumor*." Current Medical Imaging Reviews 14.4 (2018): 489-505.

[4] Coupé, Pierrick, et al. "*Robust Rician noise estimation for MR images*." Medical image analysis 14.4 (2010): 483-493.

[5] Kalaiselvi, T., S. KarthigaiSelvi, and M. Vinothini. "*Investigation of Wavelet Applications in Magnetic Resonance Imaging*." computational methods, communication techniques, and informatics: 106.

[6] WANG, CUI, CAI-XIA DENG, and ZHI-BIN HU. "*An Improved Wavelet Threshold Function And Its Application In Image Edge Detection*." 2019 International Conference on Wavelet Analysis and Pattern Recognition (ICWAPR). IEEE, 2019.

[7] Bnou, Khawla, Said Raghay, and Abdelilah Hakim. "*A wavelet denoising approach based on unsupervised learning model."* EURASIP Journal on Advances in Signal Processing 2020, no. 1 (2020): 1-26.

[8] Ferzo, Barwar Mela, and Firas Mahmood Mustafa. "*Image Denoising in Wavelet Domain Based on Thresholding with Applying Wiener Filter*." In 2020 International Conference on Computer Science and Software Engineering (CSASE), pp. 106-111. IEEE, 2020.

[9] Chang, S. Grace, Bin Yu, and Martin Vetterli. "*Adaptive wavelet thresholding for image denoising and compression*." IEEE transactions on image processing 9.9 (2000): 1532-1546.

[10] Blu, Thierry, and Florian Luisier. "*The SURE-LET Approach to image denoising*." IEEE Transactions on Image Processing 16.11 (2007): 2778-2786.

[11] Dengwen, Zhou, and Cheng Wengang. "*Image denoising with an optimal threshold and neighbouring window*." Pattern Recognition Letters 29.11 (2008): 1694-1697.

[12] Buades, Antoni, BartomeuColl, and Jean-Michel Morel. "*A review of image denoising algorithms, with a new one.*" Multiscale Modeling & Simulation 4.2 (2005): 490-530.

[13] Kumar, BK Shreyamsha. "*Image denoising based on non-local means filter and its method noise thresholding*." Signal, image, and video processing 7.6 (2013): 1211-1227.

[14] Kalaiselvi, T., and S. KarthigaiSelvi. "*A novel wavelet thresholding technique to denoise magnetic resonance image*." International journal of applied engineering research 10 (2015): 76.

[15] Sweldens, Wim. "*The lifting scheme: A custom-design construction of biorthogonal wavelets.*" Applied and computational harmonic analysis 3.2 (1996): 186-200.

[16] Liu, Zhaohua, Yang Mi, and Yuliang Mao. "*Improved Real-time Denoising Method Based on Lifting Wavelet Transform."* Measurement Science Review 14.3 (2014): 152-159.

[17] Sweldens, Wim. "*The lifting scheme: A construction of second-generation wavelets.*" SIAM Journal on mathematical analysis 29.2 (1998): 511-546.

[18] Koay, Cheng Guan, and Peter J. Basser. "*Analytically exact correction scheme for signal extraction from noisy magnitude MR signals.*" Journal of magnetic resonance 179.2 (2006): 317-322.

[19] Golilarz, NoorbakhshAmiri, and Hasan Demirel. "*Image denoising using un-decimated wavelet transform (UWT) with soft thresholding technique.*" 2017 9th International Conference on Computational Intelligence and Communication Networks (CICN). IEEE, 2017.

[20] Chaudhury, Kunal N., and Amit Singer. "*Non-local Euclidean medians*." IEEE Signal Processing Letters 19.11 (2012): 745-748.

[21] Tan, Lizhe, and Jean Jiang. Digital signal processing: fundamentals and applications. Academic Press, 2018.

[22] Rasheed, Asmaa Hameed, and Haneen Mohammed Hussein. "*Effect of different window size on median filter performance with variable noise densities.*" International Journal of Computer Applications 178.2 (2017): 22-27.

[23] BrainWeb: Simulated Brain Database (mcgill.ca)

[24] Rajkumar, S., and G. Malathi. "*A comparative analysis of image quality assessment for real-time satellite images*." Indian J. Sci. Technol 9 (2016).

[25] Kalaiselvi, T., R. Vasanthi, and P. Sriramakrishnan. "*A Study on Validation Metrics of Digital Image Processing.*" computational methods, communication techniques and informatics (2017): 396.

[26] Sadiq, Bashir Olaniyi, S. M. Sani, and S. Garba. "*Edge detection: A collection of pixel based approach for colored images*." arXiv preprint arXiv:1503.05689 (2015).

[27] Maini, Raman, and Himanshu Aggarwal. "*Study and comparison of various image edge detection techniques*." International journal of image processing (IJIP) 3.1 (2009): 1-11.

***